14th IEA Heat Pump Conference
15-18 May 2023, Chicago, Illinois

Simulation-assisted development of a mini-split air-to-water façade-integrated heat pump for minimal invasive renovations

William Monteleone[a*], Fabian Ochs[a]

[a]Unit for Energy Efficient Building, University of Innsbruck, Technikerstraße 13, 6020 Innsbruck, Austria

Abstract

One of the challenges in renovated multi-apartment buildings is the upgrade or substitution of existing systems delivering space heating (SH), domestic hot water preparation (DHW) and cooling (SC). Construction and installation works are complex and their related costs are high. The European heat pump market currently lacks compact and cost-effective solutions for minimally invasive, so-called serial renovations, which at the same time exhibit high efficiency, an aesthetically pleasing design and low sound emissions. Façade-integrated decentralised small-scale heat pumps (HP) are regarded as a promising solution to increase the general acceptance for flat-wise heating solutions. Because of the compact design, they require a deeper investigation of the fluid-dynamics within the outdoor unit (evaporator) to guarantee an adequate efficiency of the final product. Based on these considerations, a mini-split air-to-water façade-integrated HP for DHW was developed. The design of the outdoor unit was optimised by means of computational fluid-dynamics simulations (CFD) and the overall efficiency evaluated through refrigerant cycle and system simulations. To conclude, the prototype was tested dynamically in a double-room climate chamber with controlled indoor and outdoor temperature conditions.

© HPC2023.
Selection and/or peer-review under the responsibility of the organizers of the 14th IEA Heat Pump Conference 2023.

Keywords: Heat pumps; serial renovation;, alternative refrigerants; façade integration

1. Introduction and state-of-the-art

The European Building Performance Directive (EPBD) 2018/844 [1] stated the commitment of the European Union (EU) to the development of a sustainable, energetically secure and decarbonized energy system, along with a full decarbonization of the building stock by 2050, 35% of which older than 50 years old [2]. The new EPBD indicates also that EU member countries should submit national building renovation strategies within the National Energy and Climate Plans (NECPs) including roadmaps to phase out fossil-based systems supplying heating and cooling by 2040 at the latest. In order to achieve the full decarbonization of the building sector, an improved average yearly renovation rate of 3% is needed (compared to the actual 1%) along with a cost-effective transformation of existing buildings into nearly-zero energy buildings (nZEBs) [3]. Independently from how a carbon neutral energy system will be realized in the future, it is no doubt that HPs will play a crucial role in a sustainable and efficient transformation in the heating, cooling and DHW preparation of buildings [4]. During the renovation of multi-apartment buildings, a complete upgrade or substitution of the existing centralized systems delivering the SH, SC and DHW demands is frequently not possible for techno-economic reasons, among others high investment costs and high degree of invasiveness. The European market offers currently different HP based solutions depending on their construction type [5]:

a) Internal monoblock with integrated hot water storage;
b) Internal monoblock with integrated wall-hanging hot water storage;
c) Split units;
d) DHW HP with integrated or separated hot water storage.

* Corresponding author. Tel.: +43 512 507 63661
E-mail address: william.monteleone@uibk.ac.at .

Split units (air-to-air or air-to-water) are already a standardized product on the market and are offered in all power ranges. A couple of major drawbacks of such system are however the optically unattractive outdoor unit and the high developed sound power level during operation, ranging from 59 to 70 dB(A) for outdoor units and from 43 to 65 dB(A) for the internal module [5,6]. Accordingly, the European market does not yet offer compact, modular and silent split HP solutions with an aesthetically pleasing design of the outdoor unit. Innovative decentral façade-integrated small-scale HP solutions would guarantee a substantial space saving and a high degree of prefabrication, minimizing thus the total investment costs. Additionally, reduced sound emissions should improve their overall acceptance. Within the FFG (Austrian Research Promotion Agency) funded research projects FitNeS and PhaseOut a mini-split air-to-water façade-integrated HP for DHW with a design heating power of 1.5 kW was developed by means of coupled simulation and experimental work to cover an important gap on the wide renovation market and enhance serial renovation in multiple-family buildings. The design and the optimization of the outdoor unit was performed through CFD, refrigerant cycle and system simulations. To supply a proof-of-concept and to verify the efficiency of the developed design, a prototype was tested dynamically with water tapping profiles according to EN 16147 [7] in a double-room climate chamber with controlled indoor and outdoor temperature conditions.

2. Highlight of current research gaps and novelty of developed concept

DHW and SH in renovated buildings are mainly fossil based in continental Europe, with small differences among member countries [8], with more than half of the installed systems relying on either natural gas or oil [9]. New centralized installations are frequently not possible or possible for social, technical or economic reasons, among them high degree of invasiveness, higher investment costs, higher distribution losses and impossibility to provide step-wise renovation. District heating (DH) systems represent a real alternative only if they are already available on site, often not the case especially in densely populated areas. Additionally, the European market does not provide efficient and cost-effective sustainable alternatives to decentral gas-fired or electric boilers that require only minimal construction work. In this paper, a propane-based façade-integrated mini-split HP for the apartment-wise renovation of multiple-family buildings will be presented to tackle the absence of minimally invasive, compact and silent HP solutions on the broad market segment of the refurbishment of buildings. Since the integration takes mainly place within the insulation layer, a deep analysis of the fluid dynamics and the heat transfer is necessary. Firstly, the main boundary conditions of the CFD simulation work will be highlighted and the final design selected based on flow homogeneity, overall pressure drop, sound emissions and electric power consumption of the fans. Secondly, the theoretical performance of the refrigerant cycle will be evaluated under the assumption of uniform flow conditions. Then, the overall performance of the entire system, including the HP, the hot water storage and the fresh water station for the delivery of the DHW demand, will be investigated by means of dynamic system simulation. Lastly, the results of the testing of a prototype of mini-split HP under dynamic conditions will be presented.

3. Methodology

The analysis presented in this work follows a development and optimization approach from the component level up to the system level, as discussed also in [10] where the development of an air-to-air HP for SH is highlighted. The next sections will present the implemented research methodology, starting from the CFD-based design development of the outdoor unit with a brief mention of the criteria used to compare the evaluated designs. Then, the following section will highlight the basic assumptions of a steady-state refrigerant cycle simulation tool developed internally in the MATLAB environment [11] to produce reasonable performance maps of the to-be-developed mini-split HP under the simplifying assumption of uniform airflow. The generated performance maps will be then used as an input in the dynamic system model developed within the Simulink simulation environment [12] to perform a pre-sizing of the optimal size of the DHW storage. Consequently, the primary energy consumption of the entire system supplying the DHW demand will be assessed considering a hot water tapping profile based on the “M” profile according to [7] for a typical household of 2-3 persons. In the last section, the test setup at the University of Innsbruck used to measure the dynamic performance of the prototype will be discussed.

3.1. CFD-based design development and optimization

Several design geometries were simulated in the software ANSYS [13] with the help of the CFX solver in a first phase and pre-selected based on the following criteria:

- Flow homogeneity on the evaporator surface;
- Air-side pressure drop;

The pre-screening included geometrical designs with both axial and radial fans. Crossflow fans were not taken instead into further consideration due to space constraints in façade-integrated installations. Table 1 illustrates the simulated variants based on the geometry of the evaporator, the fan type and the position of the fans related to the evaporator.

Table 1: Overview of simulation cases to assess the optimal geometry of the outdoor unit by means of CFD simulations.

Variant number	Geometry	Type of Fan	Position of the Fans
1	Square	4 axial	Downstream
2.1	Rectangular	4 axial	Downstream
2.2	Rectangular	4 axial	Upstream
3	Rectangular	1 radial	Downstream
4	Rectangular	1 radial	Downstream

For the simulated variants, the boundary conditions highlighted in Table 2 were assumed throughout the CFD simulations:

Table 2: Boundary conditions in CFD simulations. For the simulations involving axial fans, the rotational speed was also varied between 900 rpm and 1700 rpm.

Type of Fan	Boundary Conditions	Value
Radial fans	Inlet	Total pressure = 0 Pa
	Outlet	Mass flow rate = 0.115 kg/s
Axial fans	Inlet	Static pressure = 0 Pa
	Outlet	Average static pressure = 0 Pa

The k-ε turbulence model was adopted for all simulation models, as it is generally suggested for flows over rotating geometries and baffles, as well as being a robust model with a sufficient accuracy [14]. Additionally, the walls of the fluid domain are assumed to be smooth and the velocity on the model boundaries is equal to zero (no-slip wall condition). To model the fluid interface between stationary and rotating domains, the option "Frozen rotor" was selected.

3.2. Refrigerant cycle simulation model and performance maps generation

In parallel to the selection of the optimal outdoor unit design based on the presented criteria, a refrigerant cycle analysis was executed with the purpose of:

a) Generating physics-based reasonable performance maps to be used in the dynamic system simulation in absence of measurement results;
b) Evaluate the maximum theoretical performance of the refrigerant cycle at varying boundary conditions.

The refrigerant cycle is based on propane (R290), an alternative and more sustainable refrigerant with a global warming potential (GWP) equal to 3 and ozone depletion potential (ODP) equal to zero [15]. However it has the drawback of belonging to the A3 class, thus highly flammable and with a maximum allowed refrigerant charge in Europe equal to 150 g for residential installations [16]. A pre-analysis of the performance of the refrigerant cycle, given the knowledge about the single components, is in this sense crucial. The model itself is built in a modular way, so that each component of the refrigerant cycle has its own equations, which will be highlighted in the following section along with the basic assumptions of the model.

3.2.1. Compressor model

The modelled compressor exhibits the characteristics highlighted in Table 3:

Table 3: Technical features of the compressor modelled within the refrigerant cycle simulation

Feature	Value
Compressor type	Rotary
Displacement	12.74 cm^3
Speed control	Single speed – 2900 rpm
Number of phases	1 – 230 V – 50 Hz

For the calculation of the isentropic efficiency associated to a certain pressure ratio, a fourth-order, ten-coefficients equation, depending on evaporation and condensation temperatures, was modelled based on manufacturer data:

$$\eta_{is} = f^4(\vartheta_{evap}, \vartheta_{cond}) \quad (1)$$

The refrigerant mass flow supplied by the compressor is calculated from a physical model, as discussed also in [17], described by equation (2) :

$$\dot{m}_{ref} = \eta_{vol} \frac{n_{rpm}}{60} D_c \rho_{ref,suction} \quad (2)$$

The volumetric efficiency is in turn also deducted from a theoretical model similar to the one described in [18] and [19] depending from the pressure ratio τ and accounting for any deviation from the ideal gas behavior, as depicted in (3) :

$$\eta_{vol} = 0.97 - \left[\left(\frac{Z_s}{Z_d}\right) \tau^{\frac{1}{k}} - 1\right] C_l - e_v \quad (3)$$

It is noteworthy to mention that the clearance volume of a compressor is usually not included in the technical data supplied by the manufacturer, but reasonably lies between 5 and 15 % of the total displacement [20]. Its value needs thus to be calibrated. The same procedure should be executed for the correction factor e_v, since different applications typically exhibit different deviations from the ideal gas behaviour. For the calculation of the electrical power consumption attributed to the compressor, a constant total efficiency of 95% was assumed for sake of simplicity, equal to the product of electrical and mechanical efficiencies.

3.2.2. Condenser and Evaporator models

For the sake of pre-analysis and to maintain the simplicity of the model, no detailed calculation of the heat transfer was implemented at the condenser and at the evaporator sides. It was however decided to take into account the heat exchange through the definition of a pinch point temperature difference between the refrigerant cycle and the primary side (air) as well as between the refrigerant cycle and the secondary side (water). No detailed model was introduced within the steady-state model to account for the performance drop under icing conditions. The power laws shown in the equations (4) and (5) were thus implemented, depending on heating and cooling power respectively:

$$\Delta T_{pp,cond} = \Delta T_{pp,cond,0} \left(\frac{\dot{Q}_{cond}}{\dot{Q}_{cond,0}}\right)^{n_{cond}} \quad (4)$$

$$\Delta T_{pp,evap} = \Delta T_{pp,evap,0} \left(\frac{\dot{Q}_{evap}}{\dot{Q}_{evap,0}}\right)^{n_{evap}} \quad (5)$$

The parameters $\Delta T_{pp,cond,0}$, $\dot{Q}_{cond,0}$, n_{cond} as well as $\Delta T_{pp,evap,0}$, $\dot{Q}_{evap,0}$, n_{evap} are subjected to calibration procedure.

3.2.3. Expansion valve model

An isenthalpic valve model was adopted for sake of simplicity. For this reason, the condition described in (6) was applied to the model:

$$h_{in,exv} = h_{out,exv} \quad (6)$$

3.2.4. Pressure drop and heat losses model

Pressure drop can be taken into account for each component of the refrigerant cycle as a fixed value or through correlations depending on the refrigerant mass flow. The calculation is separated for each phase. Heat losses are solely assigned to the compressor shell and follow the law mentioned in eq. (7):

$$\dot{Q}_{loss} = UA_{compr} \left(\vartheta_{compr} - \vartheta_{amb}\right) \quad (7)$$

3.2.5. Basic assumptions about the refrigerant cycle

The following basic assumptions were made for the simulation of the refrigerant cycle:

Table 4: Inputs assumed for the refrigerant cycle simulation regarding superheating, subcooling, air and water volume flows.

Property	Value
Superheating	6 K
Subcooling	6 K
Air volume flow	350 m^3/ h
Water volume flow	4 liter/min

The value of subcooling usually depends, among other factors, on the actual refrigerant charge in operation within the refrigerant cycle. However, since there is actually no implemented model for the calculation of the optimal refrigerant charge, this effect was neglected throughout the refrigerant cycle simulations and a constant value was used as an input instead. Performance maps were thus generated for -15, -7, 2, 7, 10, 20 °C outdoor air temperature, as well as 35, 45, 55 °C supply water temperature.

3.2.6. Calculation assumptions and convergence criteria

The numerical model uses the heating and cooling power as iterated variables to obtain a full characterization of the refrigerant cycle in terms of pressure, enthalpy, entropy and temperature. The convergence of the model is based on the minimization of an error function, defined in equations (8), (9) and (10).

$$err_{conv} = \left|\dot{Q}_{cond} + \dot{Q}_{loss} - \dot{Q}_{evap} - \dot{Q}_{compr}\right| + err_{\dot{Q}_{evap}} + err_{\dot{Q}_{cond}} \quad (8)$$

$$err_{\dot{Q}_{evap}} = \frac{\left|\dot{m}_{ref}\,(h_{evap,out} - h_{evap,in}) - \dot{m}_{src}\,c_{p,src}\,(\vartheta_{src,in} - \vartheta_{src,out})\right|}{\dot{Q}_{evap}} \quad (9)$$

$$err_{\dot{Q}_{cond}} = \frac{\left|\dot{m}_{ref}\,(h_{cond,in} - h_{cond,out}) - \dot{m}_{sink}\,c_{p,sink}\,(\vartheta_{sink,out} - \vartheta_{sink,in})\right|}{\dot{Q}_{cond}} \quad (10)$$

In the first part of the convergence function, the overall energy balance of the heat pump is checked, while the remaining terms proof the validity of the local energy balances for the evaporator and for the condenser.

3.3. Dynamic system modelling of hot water consumption and performance evaluation

The efficiency of the entire system supplying the DHW demand was evaluated within the simulation environment of *MATLAB* and *Simulink*, where the heat pump was modelled using the built-in model already present in the CARNOT Toolbox. The performance data is supplied by the developed refrigerant cycle simulation tool. The dynamic performance of the system was evaluated at the outdoor air temperatures of 10, 15 and 20 °C to be later compared with laboratory measurements. Four different storage tank sizes were simulated, corresponding to 90, 100, 110 and 120 liters. For sake of simplicity, the height of the storage tank was assumed to be constant and equal to 1.1 m, while the diameter of the tank increases with increasing storage volume. The overall heat transfer coefficient of the tank, including insulation, was selected such that for each storage volume it would correspond to the energy efficiency class ErP B [21]. The temperature of the technical room is constant and equal to 20 °C. Figure 1 shows a conceptual drawing of the hydraulic system supplying the DHW demand, as it was modelled within the simulation environment. Along with the HP and the DHW storage, a freshwater station was included in the simulation as well as in the reality to avoid legal and technical constraints due to legionella. The pipe lengths correspond to the lengths in the experimental setup. The simulation time corresponds to 24 hours, of which 14 and a half hours are reserved for tapping.

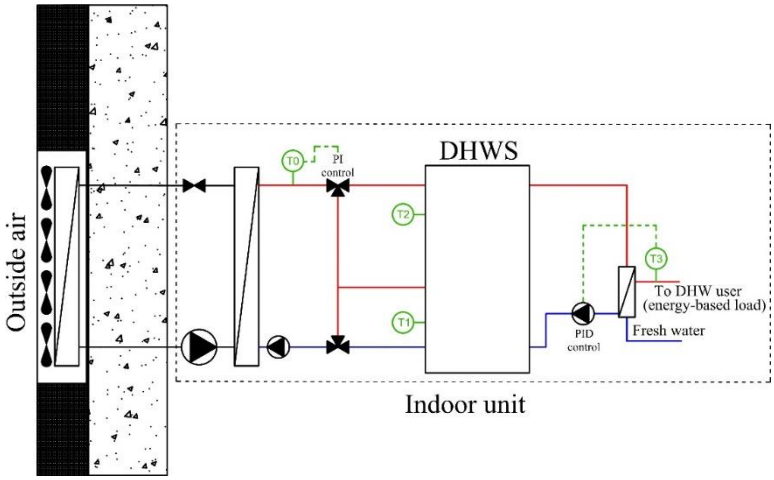

Figure 1: Schematic representation of the system supplying the DHW demand as modelled within the Simulink environment for the assessment of the optimal storage size and performance.

The entire storage tank is heated to a constant temperature equal to 55 °C. During the start-up phase of the heat pump, the temperature of the water supplied to the storage would be much lower than the actual temperature in the tank. If no additional measures were undertaken, this would result in a disturbance of the stratification of the storage and have a detrimental effect on the system performance. Thus, when the supplied water temperature is lower than 52 °C, controlled by means of the temperature sensor T0 (with an inertia of 5 seconds), the upper and lower mixing valves are closed such that water is recirculated in a loop and its temperature increases. As soon as the setpoint temperature is reached, the storage tank is loaded from above by means of fixed-value control so that a certain reserve volume can be guaranteed for short-term taps. After the reserve volume has been charged, the storage tank is also charged via the intermediate layer, whereby the fixed value control is not used here. Then the lowest part of the hot water storage tank is charged. The control of the temperature in the storage tank is performed based on a hysteresis controller coupled to the temperature sensors T1 and T2. When T2 indicates a temperature equal to the setpoint (55 °C), the heat pump is shut down. On the other hand, when T1 measures a temperature equal to 5 K lower than the setpoint (thus 50 °C), the heat pump is turned on again. On the secondary side, the rotational speed of a PID-controlled inverter-based pump is modulated in order to meet the user water temperature request, in this case 45 °C (temperature sensor T3). When the desired hot water temperature is reached, the energy control starts counting and tapping continues until the required energy has been supplied.

A tapping profile based on profile "M" according to the standard EN 16147 [7] was taken into consideration for the simulations, in which two major taps (10 liter/min) take place at 07:15 and 21:30 (i.e. shower in the morning and in the evening). Each simulation starts with a completely charged storage. Minimum and maximum operational time intervals of, respectively 5 and 80 minutes are assumed. For air temperatures lower than 7 °C, a 10 minutes stop interval is considered every 80 minutes to take into account for deicing cycles. However, the additional electric power consumption for deicing, for which calculation a dedicated model would be needed, is not taken into account.

The performance of the system is evaluated through the definition of a coefficient of performance (COP) for the entire system as follows:

$$COP_{sys} = \frac{Q_{DHW}}{Q_{el}} \qquad (11)$$

3.4. Laboratory testing and proof-of-concept

The laboratory infrastructure was used first to compare the electric power consumption and the sound power level of different fan configurations for the outdoor unit and then to test the dynamic performance of a developed prototype of mini-split façade-integrated HP for DHW preparation. To test the electric power consumption as well as the sound power level of the fan configurations, the test rig described in Figure 2 has been set up. The pressure conditions upstream of the fans (1) is imposed by means of a PI controlled ventilation flap. In the same way the pressure difference with the environment downstream of the fans (2) was equaled to zero to replicate outflow in the environment by means of a support fan. The rotational speed of the fans is

either controlled by a PWM module for the axial fans and via a 0-10 V control signal for the radial fans. Air volume flow is measured by means of a hot-wire anemometer (3). For acoustical measurements, the channel downstream of the fans must be opened and the sound power level of the fans assessed according to [22] and [23]. On the other hand, to assess the dynamic performance of the split HP, a double room climate chamber was used. The cold room was reserved to the installation of the outdoor unit of the HP, while the ambient room was dedicated to the indoor element. The temperature in each room is controlled by means of brine-to-air and water-to-air heat exchangers. With the current system configuration, it was possible to reach a minimum outdoor air temperature of 10 °C. A conceptual scheme of the test-rig for the assessment of the dynamic performance of the mini-split HP is depicted in Figure 3. Water withdrawal is controlled by means of a magnetic 2-way valve, the withdrawn volume flow being measured by a magnetic flow meter (MFM). Since the cold water temperature cannot be directly controlled, a flush valve is opened intermittently to keep the cold water temperature as constant as possible. A flush valve is also provided on the hot water side to energetically empty the hot water storage and cool it down approximately to cold-water temperature (i.e. for the measurement of the losses attributed to the DHW storage). The temperature in the storage is measured by means of three Pt100 temperature sensors, positioned respectively at 9 cm, 40 and 70 cm from the top cover of the hot water storage. The water supply and return temperatures are also measured and logged. Thus, the prototype of split-type heat pump was tested at outdoor air temperatures of 10, 15, 20 °C under intermittent tapping (M profile, see also [7]). A temperature of 45 °C was considered as minimum comfort condition for the water supplied to the DHW user. In order to allow for longer measurement stints, a hot water storage size of 120 liters was chosen. The total measurement time corresponds to the simulation time where the water withdrawal is different from zero.

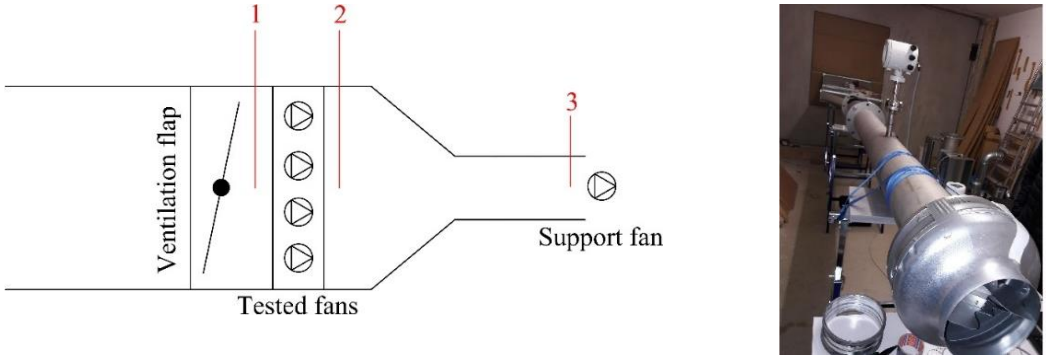

(a) (b)

Figure 2: Test rig set up for the determination of fan power consumption and sound power level. (a) Conceptual scheme and (b) photo of the actual test rig.

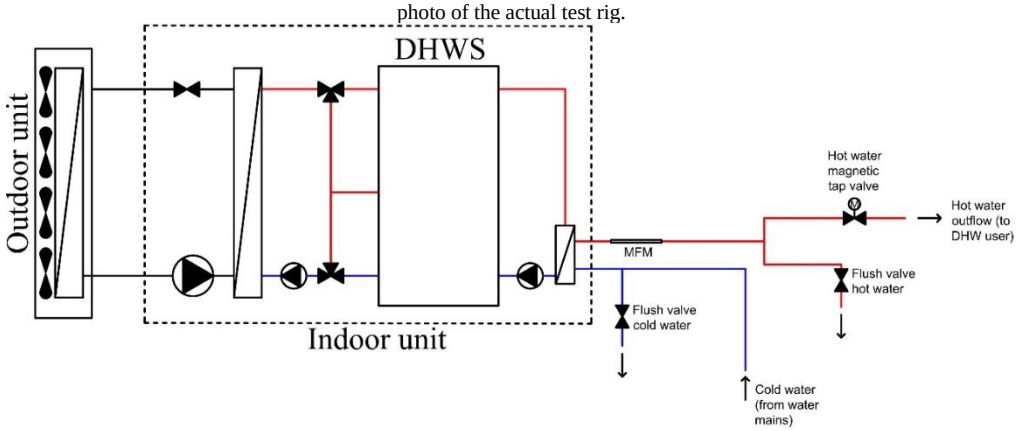

Figure 3: Test rig setup for the measurement of the dynamic performance of the system supplying the DHW demand.

4. Results and Discussion

4.1. CFD-based design development and optimization

The CFD- based pre-analysis yielded the design shown in Figure 4, involving four parallel axial fans (shown in green) and an evaporator tilted of 30° (depicted in red) compared to the inflow direction. The advantage of

axial fans over radial fans was determined with the help of the measurements of the electric power consumption as well as of the sound power level, which will be presented in a later section.

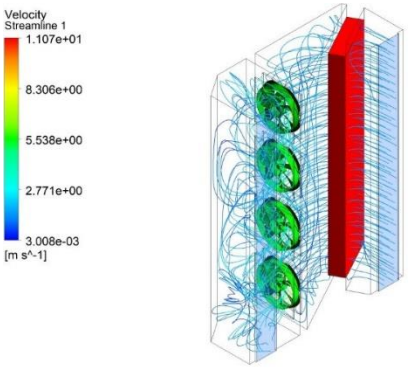

Figure 4: Final design of the outdoor unit featuring four axial fans, flow pattern simulated within the CFD software.

4.2. Refrigerant cycle simulation model and performance maps generation

The refrigerant cycle model presented in section 3.2 produced the performance maps depicted in Figure 5(a) to (d) for a split-type heat pump, with air temperature varying from -15 to 20 °C and supply water temperature of 35, 45 and 55 °C:

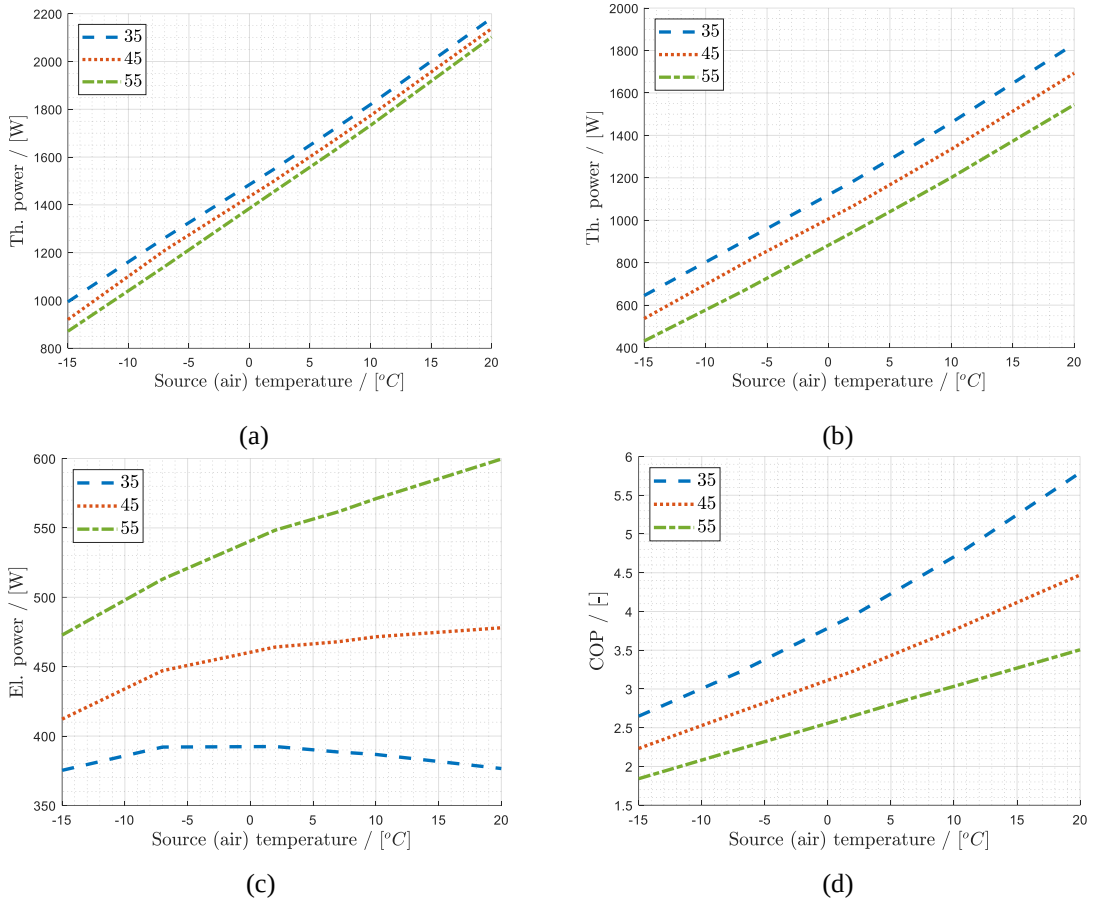

Figure 5: Simulated performance data of a split-type air-to-water heat pump to be used as input for the dynamic system simulation. (a) Heating power, (b) Cooling power, (c) Electric power consumption, (d) Coefficient of Performance with source temperatures ranging from -15 to 20 °C and supply water temperatures of 35, 45 and 55 °C.

As it is possible to discern from Figure 5(a), the design heating power of 1.5 kW at the design conditions of 7 °C air temperature, 55 °C supply water temperature is theoretically guaranteed. The generated performance

data were thus us as an input for the heat pump model in Simulink/CARNOT to investigate the dynamic performance of the entire system.

4.3. Dynamic system modelling of hot water consumption and performance evaluation

The system was simulated within the Simulink environment for multiple storage sizes at the outdoor air temperatures of 10, 15 and 20 °C. Table 5 reports the results in a concise and more compact way for the different temperatures and a storage size of 90 liters, while Table 6 summarizes the results for a storage size of 120 liters. The results show thus, that considering equal outdoor air temperature conditions, a compact 90 liters storage would be sufficient to fulfill the domestic hot water demand of a small family. The adoption of a larger storage size brings an additional 4 to 7 % performance improvement, due to the reduced switch-on frequency in the larger storage size and therefore to the comparatively lower power consumption.

Table 5: Summary of simulation results for a storage size of 90 liters and varying outdoor air temperature.

Temperature [°C]	Q_{DHW} [kWh]	Q_{el} [kWh]	COP_{sys}[-]
10	6.05	2.02	2.99
15	6.05	1.88	3.22
20	6.05	1.76	3.43

Table 6: Summary of simulation results for a storage size of 120 liters and varying outdoor air temperature.

Temperature [°C]	Q_{DHW} [kWh]	Q_{el} [kWh]	COP_{sys}[-]
10	6.05	1.88	3.22
15	6.05	1.81	3.35
20	6.05	1.68	3.61

4.4. Laboratory testing and proof-of-concept

Figure 6(a) and (b) highlight the measured sound power level and the electric power consumption for four axial fans and a single radial fan. The tests show that axial fans might be more favorable than radial one, both in terms of sound emissions and in terms of electric power consumption, if the pressure drop attributed to the inflow geometry and the evaporator can be constrained to values lower than 25 Pa. The measured total pressure drop combination of inflow geometry and evaporator in the prototype at the design airflow rate was of 9.8 Pa, confirming the choice of 4 axial fans in spite of radial fans. Figure 7 shows finally the measurement results of the prototype under dynamic conditions. Generally, it is possible to conclude that the minimum comfort requirement is always guaranteed and the minimum temperature is always supplied to the DHW user. The difference between measured and simulated performance, as highlighted by Table 6 and Table 7, is to be attributed to a higher measured storage heat loss coefficient in the experimental specimen, about 2 to 3 times higher than the simulated one due to improper insulation installation and excessive convection within the indoor unit housing the DHW storage.

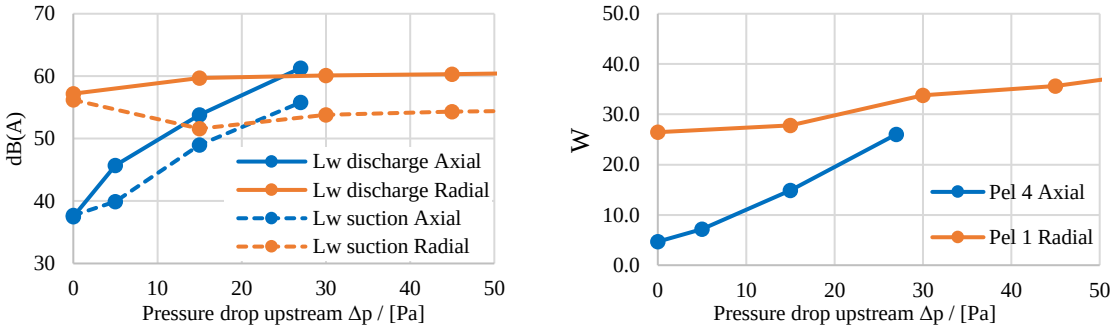

(a) (b)

Figure 6: (a) Measured sound power levels (A-corrected) on discharge and suction sides for 4 axial fans and 1 radial fan at 350 m^3/h air volume flow and (b) measured electric power consumption for 4 axial fans and 1 radial fan at varying pressure drop conditions.

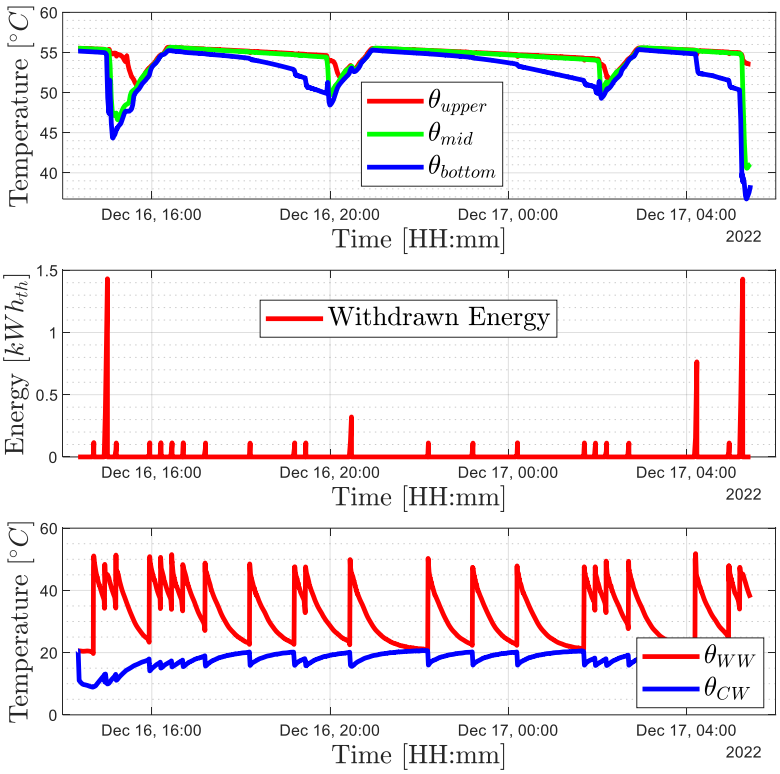

Figure 7: Measurement results of a split-type heat pump under dynamic test conditions (M standard tapping profile) and 10 °C outdoor air temperature. From the top: measured storage temperatures, withdrawn tapped energy, tapped warm and cold water temperatures. The measured storage temperatures refer to the sensors positions indicated in section 3.4.

Table 7: Summary of measurement results for a prototype of a split-type heat pump tested in a double room climate chamber under intermittent tapping and varying outdoor air temperature.

Temperature [°C]	Q_{DHW} **[kWh]**	Q_{el} **[kWh]**	COP_{sys}**[-]**
10	6.05	2.16	2.80
15	6.05	2.07	2.92
20	6.04	1.96	3.09

5. Conclusions and outlook

Decentral heat pump solutions could play a major role in the upcoming years on the renovation market. In order to save space and for sake of cost-effectiveness, one alternative and more sustainable solution to decentral gas or electric boilers is a façade-integrated split air-to-water heat pump. This work has focused on the presentation of a general procedure on how to develop efficient small-scale heat pumps in narrow environments and has given proof of the potential of such solutions. A prototype of a propane-based mini-split air-to-water heat pump was thus conceived by means of CFD, refrigerant cycle and system simulations and tested later dynamically under varying tapping conditions. The fluid-dynamics based pre-analysis has highlighted in axial fans a more favorable alternative in compact installations, due also to their lower sound emissions and lower power consumption. Additionally, system simulations have also remarked that a 90 liters storage would be sufficient to satisfy the DHW demand of a small household (2-3 people) and that slight improvements are seen for larger storage sizes. The analysis must be however extended to lower outdoor air temperatures, for which a correct modelling of ice formation and de-icing is necessary. Laboratory measurements have also shown a performance gap between the simulation performance data and the measured ones. This discrepancy was traced back to a higher measured storage heat loss coefficient in the tested HP due to improper insulation installation and excessive convection within the indoor unit. Such drawbacks will require a complete redesign of the indoor unit. Furthermore, the possibility of supplying the SH demand depending on the delivery system will be assessed for a demonstration building. In this case the condenser of the HP would be connected directly with the radiator loop or floor heating.

Nomenclature

C_l	Clearance volume of the compressor
COP_{sys}	System coefficient of performance
D_c	Displacement of the compressor
e_v	Correction coefficient for non-ideal gas behavior
h	Enthalpy
k	Isentropic expansion factor
$\dot{m}_{ref}$	Refrigerant mass flow
n_{rpm}	Rotational speed of the compressor
$\dot{Q}$	Thermal power
Q_{DHW}	Delivered energy to the DHW user
Q_{el}	Electrical energy supplied to the system for the operation of the heat pump and the auxiliaries
UA_{compr}	Compressor shell overall heat transfer coefficient
z_d	Compressibility factor of the refrigerant at discharge port
z_s	Compressibility factor of the refrigerant at suction port
ΔT	Temperature difference
η_{is}	Isentropic efficiency
η_{vol}	Volumetric efficiency
ϑ_{amb}	Technical room temperature
ϑ_{compr}	Compressor shell temperature
$\rho_{ref,suction}$	Refrigerant suction gas density
τ	Compression ratio

Acronyms

CFD	Computational Fluid Dynamics
compr	Compressor
cond	Condenser
DH	District Heating
DHW	Domestic Hot Water
EPBD	European Building Performance Directive
evap	Evaporator
exv	Expansion Valve
GWP	Global Warming Potential
HP	Heat Pump
NECP	National Energy and Climate Plan
nZEB	Nearly Zero Energy Buildings
ODP	Ozone Depletion Potential
Pp	Pinch Point
ref	Refrigerant
SC	Space Cooling
SH	Space Heating

Acknowledgements

This work is part of the research projects *FitNeS* (Nr. 867327) and *PhaseOut* (Nr. 999895470) funded by FFG (Austrian Research Promotion Agency) within the *Stadt der Zukunft* research program. Special thanks to the project partners Drexel und Weiss, Drexel Reduziert, Element Design, Kulmer Holzbau, Winter, Rothbacher and IIG.

References

[1] European Commission, Directive (EU) 2018/844 of the European Parliament and of the Council of 30 May 2018 amending Directive 2010/31/EU on the energy performance of buildings and Directive 2012/27/EU on energy efficiency, Off. J. Eur. Union. 156 (2018) 1–17. https://eur-lex.europa.eu/legal-content/EN/TXT/PDF/?uri=CELEX:32018L0844&from=EN.

[2] European Commission, Factsheet - Energy Performance of Buildings, (2021) 3. https://ec.europa.eu/commission/presscorner/detail/pt/fs_21_3673.

[3] EU, COMMISSION RECOMMENDATION (EU) 2019/786 of 8 May 2019 on building renovation, Off. J. Eur. Union. 18 (2019) 75. https://op.europa.eu/pt/publication-detail/-/publication/4a4ce303-77a6-11e9-9f05-01aa75ed71a1/language-en.

[4] H.-M. Henning, A. Palzer, Energiesystem Deutschland 2050, Fraunhofer-Institut Für Solare Energiesysteme ISE. (2013) 46.

[5] F. Ochs, D. Siegele, D. Jähnig, C. Rohringer, T. Calabrese, R. Pfluger, C. Fink, Sanierung von Mehrfamilienhäusern mit kleinen Wohnungen – Kostengünstige technische Lösungsansätze für Lüftung, Heizung und Warmwasser, 2020.

[6] M. Vukits, A.M. Fulterer, F. Ochs, D. Jähnig, A. Wegener, D. Siegele, E. Sibille, R. Pfluger, A. Sief, Bericht zum Stand des Wissens Lüftung, Wärmepumpen und Kompaktgeräte - Projekt SaLüH, (2018).

[7] DIN EN 16147, Heat pumps with electrically driven compressors - Testing, performance rating and requirements for marking of domestic hot water units, 2017. https://doi.org/https://dx.doi.org/10.31030/2513808.

[8] P. Biermayr, C. Dißauer, M. Eberl, M. Enigl, H. Fechner, B. Fürnsinn, M. Jaksch-Fliegenschnee, K. Leonhartsberger, S. Moidl, E. Prem, C. Schmidl, C. Strasser, W. Weiss, M. Wittmann, P. Wonisch, E. Wopienka, Innovative Energietechnologien in Österreich - Marktentwicklung 2021, Nachhalt. Wirtschaften. 21b (2022) 18–275. https://nachhaltigwirtschaften.at/de/iea/publikationen/markterhebungen.php.

[9] IEA, Austria 2020: Energy Policy Overview, Int. Energy Agency. (2020). https://www.iea.org/reports/austria-2020.

[10] F. Ochs, W. Monteleone, G. Dermentzis, D. Siegele, C. Speer, Compact Decentral Façade-Integrated Air-to-Air Heat Pumps for Serial Renovation of Multi-Apartment Buildings, Energies. 15 (2022). https://doi.org/10.3390/en15134679.

[11] Mathworks, MATLAB, (2022). https://de.mathworks.com/products/matlab.html.

[12] E. Leonardi, D. Siegele, carnotUIBK Toolbox for MATLAB Simulink, (2018). https://www.uibk.ac.at/bauphysik/forschung/carnotuibk/index.html.en.

[13] Ansys, Ansys 19.2, (2022). https://www.ansys.com/.

[14] C. Abeykoon, Compact heat exchangers – Design and optimization with CFD, Int. J. Heat Mass Transf. 146 (2020) 118766. https://doi.org/10.1016/j.ijheatmasstransfer.2019.118766.

[15] Z. Yang, B. Feng, H. Ma, L. Zhang, C. Duan, B. Liu, Y. Zhang, S. Chen, Z. Yang, Analysis of lower GWP and flammable alternative refrigerants, Int. J. Refrig. 126 (2021) 12–22. https://doi.org/10.1016/j.ijrefrig.2021.01.022.

[16] D. Colbourne, K.O. Suen, T.-X. Li, I. Vince, A. Vonsild, General framework for revising class A3 refrigerant charge limits – a discussion, Int. J. Refrig. 117 (2020) 209–217. https://doi.org/10.1016/j.ijrefrig.2020.04.024.

[17] Institution of Mechanical Engineers, 8th International Conference on Compressors and their Systems, Woodhead Publishing, 2013.

[18] B. Guo, W.C. Lyons, A. Ghalambor, Petroleum Production Engineering, A Computer-Assisted Approach, 2007. https://doi.org/10.1016/B978-0-7506-8270-1.X5000-2.

[19] K. Arnold, M. Stewart, Surface Production Operations: Design of Gas-Handling Systems and Facilities, 1999. https://doi.org/10.1016/b978-0-88415-822-6.x5000-4.

[20] A. Kayode Coker, Ludwig's Applied Process Design for Chemical and Petrochemical Plants, 2013. https://doi.org/10.1016/c2009-0-27268-0.

[21] European Parliament, Directive 2009/125/EC of the European Parliament and of the Council of 21 October 2009 establishing a framework for the setting of ecodesign requirements for energy-related products (recast) (OJ L 285 31.10.2009, p. 10), Off. J. Eur. Union. (2009) 1–40. http://data.europa.eu/eli/dir/2009/125/2012-12-04.

[22] ISO 9614-1:1993 - Determination of sound power levels of noise sources using sound intensity - Part 1: Measurement at discrete points, 1993.

[23] ISO 9614-2:1996 — Determination of sound power levels of noise sources using sound intensity — Part 2: Measurement by scanning, 1996.